



ELSEVIER

Contents lists available at ScienceDirect

Materials Letters

journal homepage: www.elsevier.com/locate/matlet

Inkjet-printed bifunctional carbon nanotubes for pH sensing

Yiheng Qin^{a,1}, Hyuck-Jin Kwon^{a,1}, Ayyagari Subrahmanyam^b, Matiar M.R. Howlader^a, P. Ravi Selvaganapathy^c, Alex Adronov^b, M. Jamal Deen^{a,*}^a Department of Electrical and Computer Engineering, McMaster University, 1280 Main Street West, Hamilton, ON L8S 4K1, Canada^b Department of Chemistry, McMaster University, 1280 Main Street West, Hamilton, ON L8S 4L7, Canada^c Department of Mechanical Engineering, McMaster University, 1280 Main Street West, Hamilton, ON L8S 4L7, Canada

ARTICLE INFO

Article history:

Received 5 March 2016

Accepted 4 April 2016

Available online 8 April 2016

Keywords:

Inkjet printing

Carbon nanotubes

Printed electronics

Thin films

pH

Sensor

ABSTRACT

The monitoring of pH values of liquids for environmental, industrial, and biological applications requires sensitive, stable, compact, and easy-to-use pH sensors. Here, we develop an inkjet printing process to deposit functionalized single-wall carbon nanotubes as both electron conduction and pH sensitive layers. Doping and de-doping of the carbon nanotubes by hydronium and hydroxide ions is the primary pH sensing mechanism. Multi-pass printing is used to deposit closely packed thin films and reduce the electrode resistance for efficient electron conduction and improved pH sensitivity. The printed electrodes on glass substrates show a reproducible pH sensitivity of 48.1 mV/pH with an average response time of 7 s and a small hysteresis of 4 mV. In addition, similar pH sensing behaviors are obtained by carbon nanotubes printed on flexible polymeric substrates. The developed inkjet printing process and pH sensing electrodes provide a cost-effective solution for future electrochemical monitoring systems.

© 2016 Elsevier B.V. All rights reserved.

1. Introduction

Accurate, real-time, reliable, and inexpensive sensing of pH values of liquid is indispensable for the monitoring of environmental, industrial, and biological parameters [1]. Microfabricated potentiometric pH sensors have shown advantages of high sensitivity, good stability, small footprints, and cost-effectiveness [1]. One key component in a potentiometric pH sensor is the sensing electrode, which consists of a pH-sensitive surface and an electron-conductive underlayer. For the pH-sensitive material, carbon nanotubes (CNTs) are attractive because of their high mechanical stability, large surface-to-volume ratio, mass production capability, ease of chemical functionalization, and tunable electrical properties [2]. Also, the Fermi level of the SWCNTs can be adjusted by doping/de-doping using the hydronium/hydroxide ($\text{H}_3\text{O}^+/\text{OH}^-$) ions in the surrounding solutions [3]. These features allow CNT-based pH sensors to exhibit a wide sensing range (pH=1–13) [4], high sensitivity (59 mV/pH) [3], fast response (< 10 s) [5], and long lifetime (> 120 days) [6].

The application of CNTs in pH sensors is restricted by their patterning. Previously, pH sensors based on unpatterned [7], physical-mask-patterned [3,8], and drop-cast [9] CNTs were

reported. Unpatterned CNTs increased sensor dimensions; patterning using physical masks was complicated and costly; drop-casting processes were non-reproducible. Thus, alternative patterning techniques should be employed. One solution is to use the facile, reproducible, and low-cost inkjet printing technology, which simultaneously deposits and patterns solution-based materials without using physical masks [10]. Although inkjet printing of CNTs has been demonstrated in many applications [11], pH sensors using inkjet-printed CNTs have not been reported.

On the other hand, electron-conductive layers in potentiometric sensors are normally noble metal films or macro carbon electrodes [1], which are different from most pH sensitive materials. Hence, multiple steps are needed for depositing the sensing and electron-conductive layers, resulting in costly and difficult-to-fabricate devices [12]. To address this issue, CNTs can be used since they are both electrically conductive [13] and pH sensitive. In future, CNTs can also be deposited on polymeric substrates for low-cost pH monitoring systems.

Here, we report the inkjet printing of single-wall CNT (SWCNT)-based potentiometric pH sensing electrodes. The printed SWCNTs play a dual role for both electron conduction and pH sensing. The electrical resistance of the SWCNT electrode is reduced by multi-pass printing. The low-resistance electrode exhibits a reproducible pH sensitivity, fast response, small hysteresis, and good stability.

* Corresponding author.

E-mail address: jamal@mcmaster.ca (M.J. Deen).¹ These authors contributed equally to this work.

2. Experimental details

The SWCNT ink (~ 2 g/L, PD1.5L1-5-COOH, NANOLAB) consists of chemical-vapor-deposition-grown SWCNTs that have been treated with concentrated sulfuric/nitric acid at reflux to produce carboxyl groups ($-\text{COOH}$) functionalized SWCNTs (SWCNT-COOH). The ink was filtered using a membrane filter ($5\ \mu\text{m}$ pore size, SMWP04700, EMD Millipore) and sonicated ($70\ \text{W}$, $25\ ^\circ\text{C}$) for 1 h before inkjet printing (LP50, Meyer Burger) using a piezoelectric printhead (SE-128 AA, Fujifilm). The printing was performed using the built-in waveform with a nozzle temperature of $30\ ^\circ\text{C}$, firing voltage of $100\ \text{V}$, firing frequency of $1\ \text{kHz}$, and printing speed of $100\ \text{mm/s}$. SWCNT ink with an area of $10\ \text{mm} \times 10\ \text{mm}$ was printed onto glass (7525M, J. Melvin Freed), polyethersulfone (PES) membranes ($0.8\ \mu\text{m}$ pore size, PES089025, Sterlitech), and liquid crystal polymer (LCP, CTX-100, Vectra) substrates. The printed films on glass and LCP were annealed on a hotplate in air at $160\ ^\circ\text{C}$ for 1 h, and for PES at $100\ ^\circ\text{C}$ for 12 h. Silver (Ag) paste (CI-1001, Engineered Materials Systems) was manually painted as electrical contacts. A polydimethylsiloxane (PDMS, Sylgard 184, Dow Corning) layer was manually dropped on top of the painted Ag for encapsulation, as shown in Fig. 1(a).

The electrode thickness was measured using a stylus profiler (Dektak XT, Bruker). A stereo microscope (AZ100, Nikon) and a scanning electron microscopy (SEM, JSM-7001F, JEOL) were used to observe the surface morphologies of the printed films. The electrode resistance was measured by a semiconductor analyzer (4200-SCS, Keithley). The potentiometric pH sensing behavior of the electrodes was evaluated following our previous report [14]. Briefly, the open-circuit voltage between a silver/silver chloride (Ag/AgCl) reference electrode (CHI111, CH Instruments) and the SWCNT electrode (both immersed in Britton-Robinson buffer solutions with $\text{pH}=3\text{--}11$) were recorded by a semiconductor analyzer (4200-SCS, Keithley).

3. Results and discussions

The low resistance of the inkjet-printed SWCNT electrodes demonstrated their electron conduction capability. A resistance of $\sim 1\ \text{M}\Omega$ was obtained for an electrode printed using 5 passes (thickness $< 20\ \text{nm}$) (Fig. 2(a)). The high resistance was caused by the thin electrodes and the disconnected SWCNT network (inset, Fig. 2(a)). For the electrode printed using 20 passes (Fig. 2(b)), many nano-voids can be observed in the printed SWCNT film. Although these nano-voids provide a large effective surface area, they deteriorate the electron conduction. When increasing to 200 passes, the nano-voids were filled up, and discrete SWCNT networks were merged (Fig. 2(c)). Thus, the SWCNT film of $\sim 700\ \text{nm}$ thick exhibited a resistivity of $\sim 1\ \text{k}\Omega$. Note that further increase in the number of printing passes would not significantly increase the electrode thickness (reduce the resistance) due to the outspreading of the printed ink.

Fig. 3(a) is the temporal pH response of a printed SWCNT

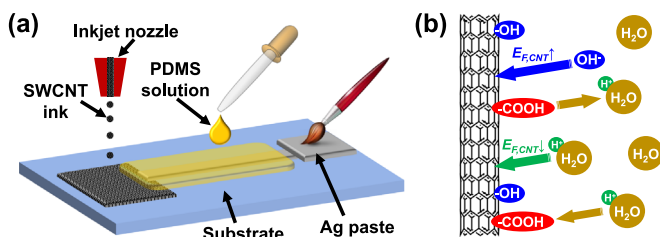


Fig. 1. (a) Schematic of the fabrication process of a SWCNT-based pH sensing electrode. (b) Schematic of the pH sensing mechanism for SWCNT-COOH.

electrode on glass (200 passes). The open-circuit voltage between the SWCNT electrode and the reference electrode decreased with the increase of the pH of the solution. This pH sensing behavior is attributed to the doping/de-doping of the SWCNTs by the $\text{H}_3\text{O}^+/\text{OH}^-$ ions close to the SWCNT surfaces in the solutions (Fig. 1(b)) [3]. In acidic solutions, the excess H_3O^+ ions are considered as p-type dopants for SWCNTs. The Fermi level of SWCNTs ($E_{F,\text{CNT}}$) shifts to a lower level upon the doping by H_3O^+ ions. Hence, the work function of the SWCNTs rises and the electrode potential is higher. In basic solutions, OH^- ions de-dope the SWCNTs, up-shift $E_{F,\text{CNT}}$, and reduce the electrode potential. Fig. 3 (a) also displays the electrode's average response time of 7 s, which proves its capability for real-time monitoring. The average hysteresis of the electrode is $\sim 4\ \text{mV}$ when the pH is cycled between 3 and 11. The fast response and small hysteresis are attributed to the closely packed SWCNT films, which reduce the length of the ion migration paths and amount of buried reaction sites in the electrodes [15].

Fig. 3(b) shows the calibration curves of the printed SWCNT electrodes for pH sensing. For the electrode printed using 200 passes, a sub-Nernst response of $48.1\ \text{mV/pH}$ was obtained. The sub-Nernst sensitivity may be caused by the $-\text{COOH}$ groups ($\sim 20\%$ coverage for the SWCNTs used in this study) at the SWCNT surfaces (Fig. 1(b)). When the solution pH changes, the $-\text{COOH}/-\text{COO}^-$ groups undergo protonation/deprotonation processes according to the equilibrium $\text{SWCNT-COOH} + \text{H}_2\text{O} \leftrightarrow \text{SWCNT-COO}^- + \text{H}_3\text{O}^+$ [16]. This reaction reduces the concentration of $\text{H}_3\text{O}^+/\text{OH}^-$ ions participating the doping/de-doping processes by 20%. Therefore, according to the Nernst equation, the sensitivity will be $47.3\ \text{mV/pH}$ (80% of the Nernstian sensitivity). This theoretical estimation agrees well with our experimental results. Although the electrode showed a sub-Nernst response, its performance was highly reproducible. The standard deviation of the sensitivity was $\sim 0.4\ \text{mV/pH}$ for 12 measurement cycles ($\text{pH}=3\text{--}11$). For the electrodes printed using 5, 20 and 80 passes, their sensitivities were 16.4, 22.6 and $36.2\ \text{mV/pH}$, respectively. The lower sensitivity is caused by the larger electrode resistance, which hinders the electron transfer. Based on these results, a Nernstian sensitivity would be realized by using non-functionalized SWCNTs and by reducing the electrode resistance to $< 1\ \text{k}\Omega$. To evaluate the stability, the printed electrodes (200 passes) were stored in ambient air at $23 \pm 2\ ^\circ\text{C}$ for 14 days. After storage, the sensitivity was $46.1\ \text{mV/pH}$, maintaining 96% of the response of newly-fabricated electrodes.

To prove the adaptability of the developed inkjet printing process with different substrates, SWCNTs were printed on PES and LCP sheets that were mounted on glass carriers (Fig. 3(c)). The resulted pH sensitivity was $45.7 \pm 0.5\ \text{mV/pH}$ and $46.1 \pm 0.8\ \text{mV/pH}$ for the electrodes on PES and LCP, respectively. These results suggest that the substrates have a minor effect on the sensing performance since the sensing behavior is mainly determined by the bifunctional SWCNTs. Therefore, CNT-based low-cost pH sensing systems printed on polymer substrates can be expected in the future.

4. Conclusions

We demonstrated the inkjet printing of functionalized SWCNTs for pH sensing purposes. The correlation between the number of printing passes and the film resistance was studied, suggesting thicker SWCNT films can be effective electron-conductive layers in potentiometric sensing electrodes. Due to the doping/de-doping of the SWCNTs in acidic and basic solutions, a fast and stable response of $48.1\ \text{mV/pH}$ was obtained for the printed SWCNTs on glass substrates. The developed inkjet printing process is simple

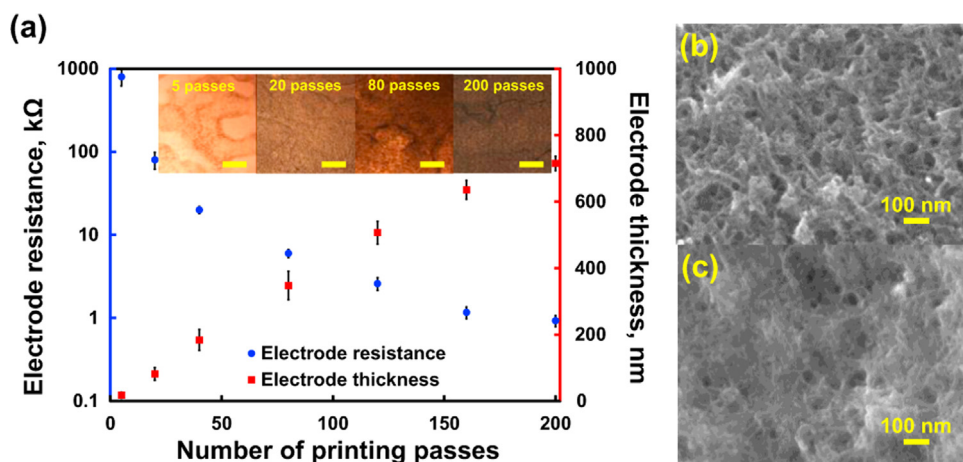


Fig. 2. (a) Electrode resistance and thickness as a function of the number of printing passes. Inset: optical microscope images of SWCNT films printed using different number of passes (scale bar: 100 μm). (b,c) SEM image of the nanostructure of a SWCNT film printed using (b) 20 passes; (c) 200 passes.

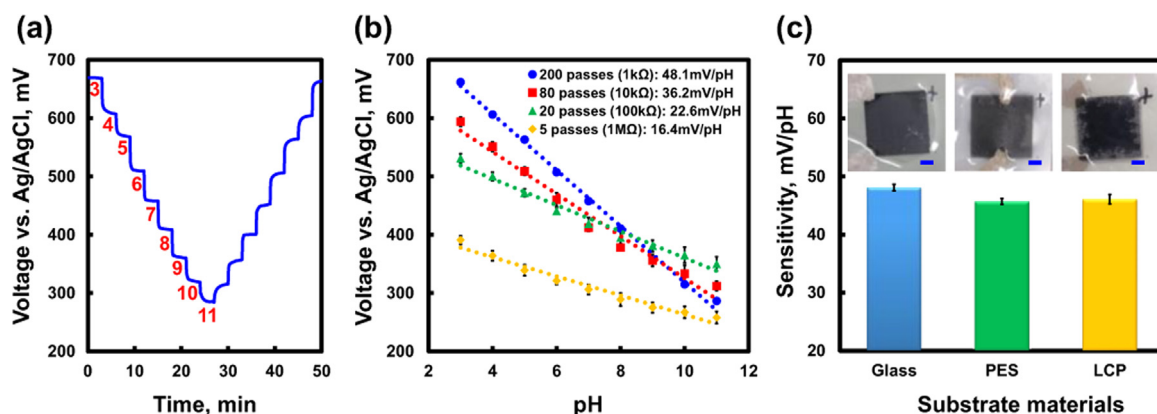


Fig. 3. (a) Temporal pH response of a printed SWCNT electrode on glass (200 passes). (b) Calibration curves of SWCNT pH sensing electrodes on glass (different numbers of printing passes). (c) pH sensitivity of SWCNT electrodes on different substrates. Inset: photographs of printed electrodes (scale bar: 2 mm).

and requires low temperatures, thus SWCNTs can be printed on polymeric substrates to facilitate their applications in low-cost electrochemical monitoring systems.

Acknowledgements

This research is supported by Discovery Grants from the Natural Science and Engineering Research Council of Canada, an infrastructure grant from the Canada Foundation for Innovation, an Ontario Research Fund for Research Excellence Funding Grant, a FedDev of Southern Ontario grant, the Canada Research Chair program, NSERC ResEau strategic network and the NCE IC-IMPACTS.

References

- [1] Y. Qin, H.-J. Kwon, M.M.R. Howlader, M.J. Deen, Microfabricated electrochemical pH and free chlorine sensors for water quality monitoring: recent advances and research challenges, *RSC Adv.* 5 (2015) 69086–69109.
- [2] L. Hu, D.S. Hecht, G. Gruner, Carbon nanotube thin films: fabrication, properties, and applications, *Chem. Rev.* 110 (2010) 5790–5844.
- [3] C.A. Li, K.N. Han, X.-H. Pham, G.H. Seong, A single-walled carbon nanotube thin film-based pH^- sensing microfluidic chip, *Analyst* 139 (2014) 2011–2015.
- [4] Z. Xu, X. Chen, X. Qu, J. Jia, S. Dong, Single-wall carbon nanotube-based voltammetric sensor and biosensor, *Biosens. Bioelectron.* 20 (2004) 579–584.
- [5] B.-R. Huang, T.-C. Lin, Leaf-like carbon nanotube/nickel composite membrane extended-gate field-effect transistors as pH sensor, *Appl. Phys. Lett.* (2011) 023108.
- [6] P. Gou, N.D. Kraut, I.M. Feigel, H. Bai, G.J. Morgan, Y. Chen, et al., Carbon nanotube chemiresistor for wireless pH sensing, *Sci. Rep.* (2014) 4468.
- [7] D. Jung, M.-E. Han, G.S. Lee, pH-sensing characteristics of multi-walled carbon nanotube sheet, *Mater. Lett.* 116 (2014) 57–60.
- [8] K. Lee, J.-H. Kwon, S. Moon, W.-S. Cho, B.-K. Ju, Y.-H. Lee, pH sensitive multi-walled carbon nanotubes, *Mater. Lett.* 61 (2007) 3201–3203.
- [9] N. Mzoughi, A. Mzoughi, Q. Gong, H. Grothe, P. Lugli, B. Wolf, et al., Characterization of novel impedimetric pH-sensors based on solution-processable biocompatible thin-film semiconducting organic coatings, *Sensor. Actuators B Chem.* 171 (2002) 537–543.
- [10] M. Singh, H.M. Haverinen, P. Dhagat, G.E. Jabbour, Inkjet printing-process and its applications, *Adv. Mater.* 22 (2010) 673–685.
- [11] K. Chen, W. Gao, S. Emaminejad, D. Kiriya, H. Ota, H.Y.Y. Nyein, et al., Printed carbon nanotube electronics and sensor systems, *Adv. Mater.* (2016), <http://dx.doi.org/10.1002/adma.201504958>.
- [12] Y. Qin, M.M.R. Howlader, M.J. Deen, Y.M. Haddara, P.R. Selvaganapathy, Polymer integration for packaging of implantable sensors, *Sens. Actuators B Chem.* 202 (2014) 758–778.
- [13] Y. Fu, Y. Qin, T. Wang, S. Chen, J. Liu, Ultrafast transfer of metal-enhanced carbon nanotubes at low temperature for large-scale electronics assembly, *Adv. Mater.* 22 (2010) 5039–5042.
- [14] Y. Qin, A.U. Alam, S. Pan, M.M.R. Howlader, R. Ghosh, P.R. Selvaganapathy, et al., Low-temperature solution processing of palladium/palladium oxide films and their pH sensing performance, *Talanta* 146 (2016) 517–524.
- [15] M. Berggren, A. Richter-Dahlfors, Organic bioelectronics, *Adv. Mater.* 19 (2007) 3201–3213.
- [16] D. Lee, T.H. Cui, pH-dependent conductance behaviors of layer-by-layer self-assembled carboxylated carbon nanotube multilayer thin-film sensors, *J. Vac. Sci. Technol. B* 27 (2009) 842–848.